Thermochimica Acta 594 (2014) 80–88

Contents lists available at ScienceDirect

Thermochimica Acta

journal homepage: www.elsevier.com/locate/tca

Non-isothermal crystallization kinetics from the melt of nanocomposites based on poly(3-hydroxybutyrate) and modified clays

D.A. D'Amico, V.P. Cyras, L.B. Manfredi *

INTEMA – Instituto de Investigaciones en Ciencia y Tecnología de Materiales, Facultad de Ingeniería, Universidad Nacional de Mar del Plata, J. B. Justo 4302, Mar del Plata 7600, Argentina

ARTICLE INFO

Article history:
Received 7 July 2014
Received in revised form 20 August 2014
Accepted 24 August 2014
Available online 27 August 2014

Keywords:
Polyhydroxybutyrate
Clay
Nanocomposites
Non-isothermal crystallization kinetics

ABSTRACT

Poly(3-hydroxybutyrate) (PHB) films and its nanocomposites were obtained by casting. Three types of modified clays were used in order to improve the compatibility with the PHB. The films were characterized determining the thermal properties and the non-isothermal crystallization kinetic parameters from the melt. No change in the melting temperature of PHB was observed with the clay addition but the T_g diminished for the nanocomposites with the clay modified by ion exchange (MI) and by acid activation (MAI) to the PHB, due to the effect of the organic modifiers.

From non-isothermal studies, it was observed a diminution of the peak of the crystallization temperature of PHB with the addition of clay at all of the cooling rates studied. The nanocomposites with MI and MAI exhibited the slowest crystallization rate among the materials, studied by the Liu–Mo model. However, the addition of the clay modified by silylation (MAGI) did not affect the crystallization rate of PHB.

Effective activation energy (E_α) of the crystallization process of PHB and the nanocomposites was calculated by the isoconversional methods of Friedman and Vyazovkin. The E_α of the PHB increased with the addition of any type of the clays studied, but the rate of crystallization was reduced.

1. Introduction

In recent years, sustainability, environmental concerns and green chemistry have played a large role in controlling the development of the next generation of materials and products. In response to increasing public awareness over the environmental hazards caused by plastics, research is underway on producing biodegradable plastic materials. Particularly, an eco-friendly alternative to this biodegradable material is poly-3-hydroxybutyrate (PHB) which is a hydrophobic and thermoplastic polyester [1–4].

It is a biopolymer accumulated by bacteria as a reserve of carbon and energy and it can be produced from renewable resources. Owing to its enzymatic synthesis, PHB has an exceptional stereochemical purity and is completely isotactic and capable of crystallizing. As a consequence, PHB is very stiff and brittle, which seriously limits its application possibilities. Its processing is difficult given that its melting point (175 °C) is slightly lower than the temperature at which it starts to degrade (185 °C) [2,5,6].

Many methods have been proposed to improve the physical properties of PHB, like the addition of fillers as reinforcing agents, such as montmorillonite. But in order to produce a clay polymer nanocomposite with improved properties it is necessary to obtain an exfoliated structure, with a complete and uniform dispersion of the clay in the polymeric matrix [7]. Nanoclay is naturally hydrophilic, whereas PHB molecules are amphiphilic–hydrophobic. So, it is necessary to use organo-modified montmorillonites in order to increase the chemical compatibility between both components improving the dispersion of clay and the final properties of the material [6,8].

The final polymer properties depend on the crystallization conditions and the addition of clay plays a significant role in affecting the PHB morphology and crystallization behavior. So, it is very useful to characterize the crystallization and structural development of PHB in clay reinforced polymer nanocomposites. From the study of the crystallization kinetics it can be determined: optimum processing temperatures, viability of manufacturing a particular part, dead time until the use of the part, etc. [9]. Non-isothermal analysis involves the study of the crystallization of the polymeric material from the melt to the solid [10].

* Corresponding author.
E-mail address: lbmanfre@fi.mdp.edu.ar (L.B. Manfredi).

http://dx.doi.org/10.1016/j.tca.2014.08.023
0040-6031/

Different methods have been developed to model the non-isothermal crystallization, which contain similarities with the models used in the solidification and crystallization of other materials. Crystallization studies generally are limited to ideal conditions, where the external conditions are constant. In such cases, theoretical analysis is relatively simple and the problems associated with cooling rates and thermal gradients within the samples are practically negligible. However, external conditions change continuously in practice making more complex of the non-isothermal crystallization process. Nevertheless, the study of the crystallization kinetics in environments which are subject to constant changes is interesting; due to the industrial processes generally take place in non-isothermal conditions. Moreover, from the scientific point of view, it may help to understand phenomena of crystallization of polymers that cannot be observed by isothermal methods due to the narrow range of temperatures at which they crystallize [9,11].

There are a variety of approaches which provide the different kinetic parameters of a crystallization process. One of these parameters is the activation energy of the process, which can be covered in different ways. All studies concerning crystallization showed that the process rate varies with temperature, resulting in a bell-shaped curve [11,12]. The characteristic shape of the curve is due to the decrease in the crystal growth rate because of the viscosity increment of the system in the temperature range close to the glass transition temperature of the polymer, and also to the lower thermodynamic driving force of crystallization when the material is near to the melting temperature [10].

It is well known that the activation energy decreases with the increase of the crystallization temperature for both processes, from the glassy state or the molten state [13]. The physical meaning of the activation energy is controversial because the crystallization rate does not obey a simple Arrhenius law. Upon solidification from the melt, the activation energy takes negative values and increases with decreasing the crystallization temperature, a typical anti-Arrhenius behavior; that is, the lower the temperature, the faster the crystallization rate [14]. The value of activation energy is equal to zero at the maximum of crystallization rate and from there, if the temperature continues to decrease, the activation energy changes sign from negative to positive. Therefore, by performing crystallization experiments at several temperature ranges different values of activation energy can be obtained. So, this parameter does not represent an energy barrier to the crystallization process, it is an effective parameter, although at times it is interpreted like this. Numerous studies erroneously implemented the definition of such effective activation energy [15–17].

Non-isothermal crystallization kinetics of PHB was previously studied [18,19]. Ziaee and Supaphol [18] found that various macrokinetic models (Avrami, Tobin, and Ozawa) were satisfactory in describing the non-isothermal melt- and cold-crystallization of PHB. The inverse half-time of crystallization and both the Avrami and the Tobin rate constants increased with increasing cooling or heating rate. For the cold-crystallization process, the Ozawa rate constant was found to increase with increasing temperature. The effective energy barrier decrease in its magnitude with increasing relative crystallinity for both the melt- and the cold-crystallization processes.

On the other hand, An et al. [19] also studied the non-isothermal crystallization of PHB ($Mw = 2.9 \times 10^5$) from the melt and the glassy state by several analysis methods. They found that the crystallization rate increases with increased heating/cooling rates, but the half-time of crystallization decreases. Additionally, the Liu–Mo kinetic parameter $F(T)$ systematically increases with a rise in the relative degree of crystallinity for non-isothermal melt and cold crystallization.

In this work, non-isothermal crystallization kinetics of nanocomposites based on PHB and organo-modified clays were investigated using differential scanning calorimetry. In order to improve the compatibility between the hydrophobic polymer matrix and the clay, three kinds of modification strategies were used on the nanofiller. Experimental data were analyzed using several reported methods, involving the isoconversional, in order to find the overall crystallization behavior of PHB from the melting state, which is very interesting prior to any attempt of melt processing. These results were analyzed to determine the influence of different types of clay on the crystallization kinetics of PHB.

2. Experimental

2.1. Materials

A biodegradable polymer, polyhydroxybutyrate (PHB) (Mn = 240,000) was kindly supplied by PHB Industrial S.A., Brazil. Montmorillonite Cloisite® Na^+ ($MCNa^+$) with a cation exchange capacity (CEC) of 92.6 meq/100 g clay was supplied by Southern Clay Products (Texas, USA). Dimethyloctadecylchlorosilane (DMOCS) and tributylhexadecylphosphonium bromide organic modifiers as well as pyridine (anhydrous, 99.8%) were purchased from Aldrich and used as received. Other solvents were purified by conventional drying and distillation procedures.

2.2. Methods of clay modification

2.2.1. Ion exchange

In this reaction hydrated cations located in the interlayer space are replaced by tributylhexadecylphosphonium bromide (TBHP). After this treatment, the basal spacing of the layers increases and the modified clay has less surface energy and hence is more compatible with hydrophobic polymers.

$MCNa^+$ was dispersed in distilled water (2.5 g of clay/100 ml water), then TBHP was added. The mixture was stirred for 4 h at 70 °C. Subsequently, the suspension was filtered on Buchner and washed three times with distilled water and ethanol. Finally, exchanged clays were dispersed in ethanol and dried in an oven at 80 °C for 24 h. This clay was denoted as MI.

2.2.2. Acid activation and ion exchange

The treatment of $MCNa^+$ with mineral acid dissolves impurities, opens the edges of the platelets, and then increases the surface area and the pore diameters. Also, exchangeable cations are replaced by protons increasing the amount of —OH groups available for further functionalization.

5 grams of $MCNa^+$ were dispersed in 200 ml of water. Then, 10 ml of H_2SO_4 were added and stirred at room temperature during 6 h, yielding a stable colloid due to increased hydrophilicity. The dispersion was centrifuged and the activated clay (supernatant) was separated. The clay was washed with 30 ml of distilled water, then stirred and centrifuged at 10,500 rpm during 10 min (in triplicate). Finally, the clay was lyophilized for 72 h. Then, the powder resultant was exchanged with the same methodology of above. This clay was denoted as MAI.

2.2.3. Silylation of MAI

The grafting of silane molecules at the hydroxyl groups present on the surface of the clay could contribute with the compatibility of the clay with the polymer matrix.

A 0.75 g portion of MAI was placed (previously dried in an oven at 110 °C) in 175 ml of butanol with 5 g of DMCOS and stirred continuously in a silicone oil bath at 100 °C. Then, 1.75 ml of pyridine was added and the mix was refluxed with constant stirring for 24 h. The modified clays were centrifuged at 10,500 rpm for 10 min. The supernatants were decanted and washed three times with butanol and once with ethanol. Finally, the grafted clays

were dispersed in 20 ml of ethanol and dried in an oven at 80 °C for 24 h. This clay was denoted as MAGI.

2.3. Preparation of PHB—layered silicate nanocomposites

Films of PHB and its nanocomposites were obtained by casting process. A homogeneous solution of PHB in chloroform was prepared by stirring at 450 rpm while heating at 60 °C, for 15 min. Then, the solution was placed on glass Petri dishes and it was allowed to evaporate at room temperature. Nanocomposites were prepared in the same way, but with the addition of a previously sonicated chloroform clay solution to the PHB chloroform solution. Nanocomposites contained 4 wt%/wt of each kind of montmorillonite. All films were stored in a desiccator at room temperature for 30 days to allow complete crystallization of PHB [6]. The film thickness of PHB and nanocomposites was 0.08 mm.

The flow diagram in Fig. 1 summarizes the preparation methods of the modified clays and nanocomposites of PHB.

2.4. Experimental techniques

2.4.1. X-ray diffraction (DRX)

The analyses of the composites were done in a X-Pert diffractometer (40 kV and 40 mA) at 2°/min with a radiation of $K_{Cu1\alpha}$ ($\lambda = 1.54$ Å), in the 1.5–60° range.

2.4.2. Thermogravimetry (TGA)

Thermal degradation measurements were carried out in a Shimadzu TG-50. Dynamic tests were performed under nitrogen environment, from ambient temperature up to 700 °C and at 10 °C/min heating rate. The organic modifier content of each type of clay was determined from the mass loss vs. temperature curve, considering the percentage of mass lost in the 120–600 °C range, where the organic modifier degradation occurs.

2.4.3. Transmission electron microscopy (TEM)

Tests were performed in a FEI Tecnai G2-20 with a filament LaB_6 using an acceleration voltage of 200 kV. The specimens were sectioned into ultra thin slices (90 nm) at room temperature, using a Cryo-Ultramicrotome Leica at −30 °C.

2.4.4. Differential scanning calorimetry (DSC)

The melting temperature and the overall crystallinity of the samples were obtained with one scan from room temperature to 200 °C at a rate of 10 °C/min under inert nitrogen flow, in a PerkinElmer Pyris 1 DSC. About 5 mg of sample was placed in an aluminum pan.

The overall crystallinity was calculated according to the following equation:

$$X_c(\%) = \frac{\Delta H_m \times (m_C/m_P)}{\Delta H_0} \times 100 \quad (1)$$

where ΔH_m is the melting enthalpy measured from heating experiments, ΔH_0 is the theoretical enthalpy of 100% crystalline PHB ($\Delta H_0 = 146$ J/g [20]), m_c is the nanocomposite weight and m_p is the weight of PHB in the nanocomposite.

Non-isothermal crystallization behavior of PHB and its nanocomposites was studied by cooling the samples from 195 °C to room temperature at constant rates of 5, 7.5, 10, 12.5 and 15 °C/min. It should be noted that it was necessary to melt the sample at 195 °C for at least 1 min to erase its previous thermal history as well as to avoid its thermal degradation, as it was found in our previous work [6].

3. Theoretical background

The relative degree of crystallinity as a function of temperature, α_T, can be formulated as:

$$\alpha_T = \frac{\int_{T_0}^{T} (dH_c/dT)dT}{\int_{T_0}^{T_\infty} (dH_c/dT)dT} \quad (2)$$

where T_0 and T_∞ denotes the temperatures at which crystallization starts and end, respectively. The crystallization temperature can be converted to crystallization time, t, using the following equation:

$$t = \frac{(T_0 - T)}{\beta} \quad (3)$$

where T_0 is the temperature at which crystallization begins (time $t = 0$), T the temperature at crystallization time t, and β is the cooling rate. The transformation from temperature to time is performed using a constant cooling rate.

The relative degree of crystallinity, α_t, is related to the crystallization time, t, according the Avrami model as:

$$\alpha_t = 1 - \exp(Z_t t^n) \quad (4)$$

$$\ln[-\ln(1 - \alpha_t)] = \ln Z_t - n \ln t \quad (5)$$

where n is the Avrami exponent and Z_t is the crystallization rate constant involving both nucleation and growth rate parameters. This theory provides useful data on the overall crystallization kinetics. The parameters, n and Z_t, can be used to interpret qualitatively the nucleation mechanism, morphology and the overall crystallization rate of the polymer.

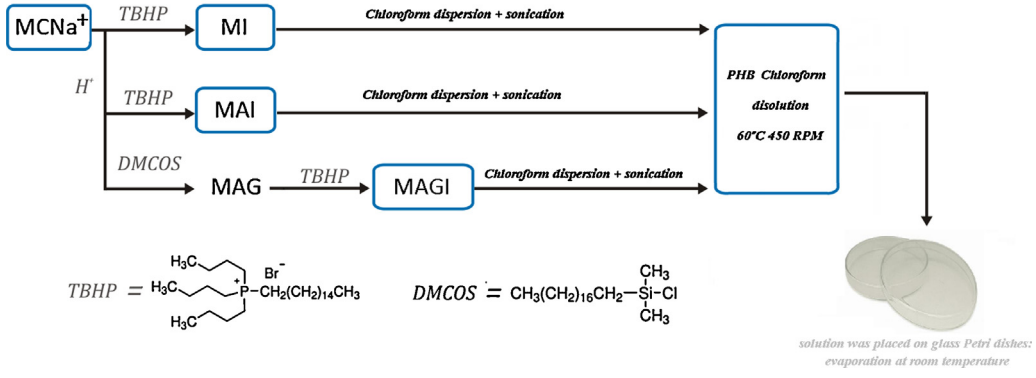

Fig. 1. Flow diagram showing the preparation methods of the modified clays and nanocomposites of PHB.

Table 1
Interlayer spacing and organic content of modified clays and nanocomposites.

Sample	d_{001} (nm)	Organic content (%)
Clay MAGI	2.18	27.0
Clay MAI	2.05	22.9
Clay MI	2.18	24.6
PHB + 4% MAGI	2.34	–
PHB + 4% MAI	2.32	–
PHB + 4% MI	2.29	–

Considering the non-isothermal conditions of the crystallization, Jeziorny [21] proposed the following form of the crystallization rate constant parameter:

$$\ln Z_c = \ln \frac{Z_t}{\beta} \tag{6}$$

Ozawa [22] extended the Avrami equation assuming that the crystallization in non-isothermal conditions is the result of an infinite number of isothermal steps. The relative degree of crystallinity can be calculated as follows:

$$\alpha_T = 1 - \exp\left[\frac{-K_T}{\beta^m}\right] \tag{7}$$

$$\ln[-\ln(1-\alpha_t)] = \ln K_T - m \ \ln \ \beta \tag{8}$$

where K_T is a cooling function related to the overall crystallization rate and m is the Ozawa exponent that depends on the dimension of crystal growth.

Liu et al. [23] combined the Avrami and Ozawa equations. Then, the expressions obtained from the combination of both models are shown in Eqs. (9–11), which give a relationship between α and t:

$$\ln Z_t + n \ \ln t = \ln K_T - m \ \ln \beta \tag{9}$$

$$\ln \beta = \frac{1}{m} \ln \left[\frac{K_T}{Z_t}\right] - \frac{n}{m} \ln t \tag{10}$$

$$\ln \beta = \ln \ F(T) - b \ln t \tag{11}$$

where the kinetic parameter $F(T) = [K_T/Z_t]^{1/m}$, represents the value of cooling rate chosen at a unit crystallization time when the systems have a defined degree of crystallinity, and b is the ratio of the Avrami exponent (n) to the Ozawa exponent (m). Plotting $\ln\beta$ vs. $\ln t$, to a certain degree of crystallinity, it is possible to determine the values of $F(T)$, from the intercept of the lines. This model was applied to a variety of nanocomposites [24–26]. The nucleation activity (ϕ) is a parameter developed by Dobreva and Gutzow [27], which estimates the variation in the tridimensional nucleation activity of a melt polymer by a filler addition. It was defined as follows:

Table 2
Thermal properties of PHB and its nanocomposites.

Material	T_m (°C)	ΔH_m (kJ/mol)	T_g (°C)	Xc (%)	ϕ
PHB	176.9	95.0	−5.8	65.1	1
PHB + 4% MI	175.0	85.8	−3.8	61.8	1.45
PHB + 4% MAI	175.1	89.0	−3.9	63.3	0.83
PHB + 4% MAGI	175.4	85.9	−5.9	61.6	0.95

$$\varphi = \left[\frac{B^*}{B}\right] \tag{12}$$

where B can be experimentally determined from crystallization tests using the following equation:

$$\ln \beta = A - \left[\frac{B^*}{\Delta T_c{}^2}\right] \tag{13}$$

where A is a constant and $\Delta T_c = T_m - T_c$ is the undercooling, with T_m the polymer melting temperature and T_c the crystallization peak temperature. B^* represents the value of B when the polymer crystallize in the presence of a filler, and B when there is no substrate. The value of ϕ increases as the nucleation activity decreases, and it can vary from 0 to 1.

It is also interesting to calculate the effective activation energy of the non-isothermal crystallization process. Friedman [28] and Vyazovkin [29] isoconversional methods were probed to be accurate mathematical approaches for evaluating this property on cooling crystallization [30].

The Friedman equation is expressed as:

$$\ln\left(\frac{d\alpha}{dt}\right)_\alpha = C - \frac{E_\alpha}{RT_\alpha} \tag{14}$$

where $(d\alpha/dt)$ is the instantaneous crystallization rate as a function of time at a given conversion α,C is a constant and, E_α and T_α are the

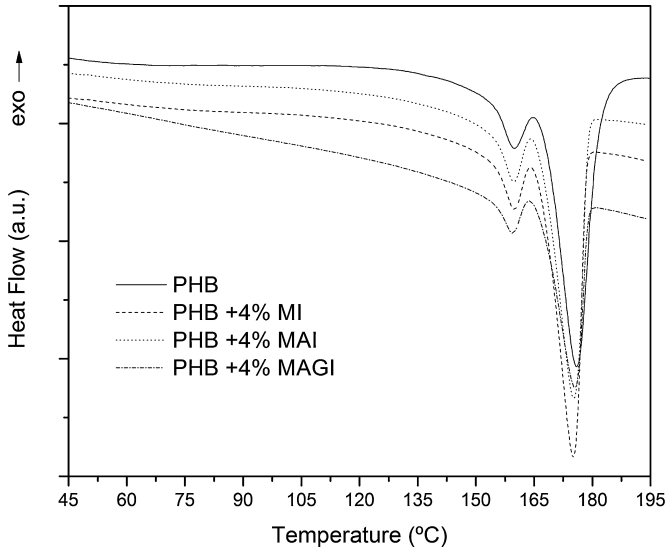

Fig. 2. DSC melting curves of PHB and its nanocomposites, at 10 °C/min.

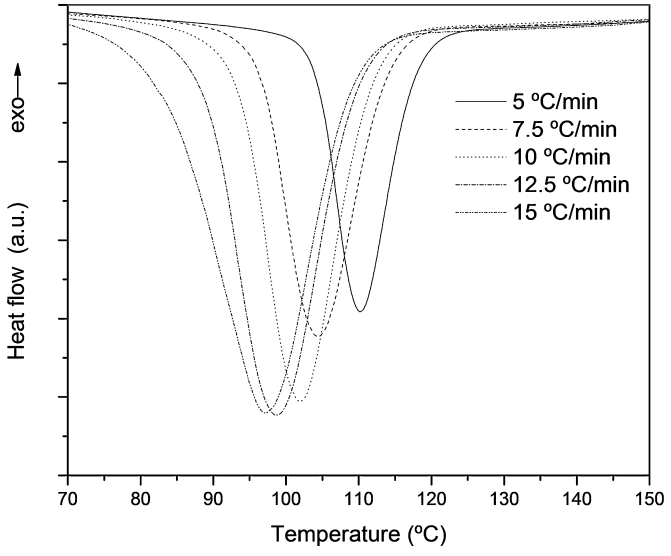

Fig. 3. DSC thermograms of non-isothermal crystallization for the PHB + 4 wt% MAI nanocomposite at various cooling rates.

effective activation energy and the temperature at a certain conversion degree, respectively. At each selected α, the value of E_α can be determined from the slope of a plot of $\ln(d\alpha/dt)$ vs. $1/T$.

Vyazovkin developed an advanced integral isoconversional method. For a series of experiments performed at different cooling rates, the E_α value can be determined by minimizing the function expressed by Eq. (15). The temperature integral (Eq. (16)) is numerically solved.

$$\zeta(E_\alpha) = \sum_{i=1}^{n} \sum_{i \neq j}^{n} \frac{J[E_\alpha, T_i(t_\alpha)]}{J[E_\alpha, T_j(t_\alpha)]} \quad (15)$$

$$J[E_\alpha, T_i(t_\alpha)] \equiv \int_{t_\alpha - \Delta_\alpha}^{t_\alpha} \exp\left[\frac{-E_\alpha}{R \times T_i(t)}\right] \times dt \quad (16)$$

where i and j denote the different thermal experiments, $\Delta\alpha$ is the conversion increment, and $J[E_\alpha, T_i(t_\alpha)]$ is the temperature integral which can be well approximated with a numeric integral [31]. Subsequently, these data are used to minimize Eq. (15) by seeking an appropriate E_α value. Repeating this minimization procedure for each α of interest, E_α as a function of α will be established.

It is also possible to analyze the spherulitic growth rate for polymer melt crystallization applying the Hoffman–Lauritzen theory, expressed by Eq. (17):

$$G = G_0 \exp\left(\frac{-U^*}{R(T - T_\infty)}\right) \exp\left(\frac{-K_g{}^*}{T\Delta T_f}\right) \quad (17)$$

where G_0 is the pre-exponential factor, U^* is the activation energy of the segmental jump, T_∞ is a hypothetical temperature at which viscous flow ceases (usually taken 30 K below the glass transition temperature, T_g), f is the corrective factor which equals $2T/(T_m + T)$, T_m is the equilibrium melting temperature, ΔT stands for the supercooling $(T_m - T)$, R is the universal gas constant and K_g is the nucleation constant associated with morphology and transition of crystals, which has the following form:

$$K_g = \frac{nb\sigma\sigma_e T_m}{\Delta h_f k_B} \quad (18)$$

where b is the surface nucleus thickness, σ is the lateral surface free energy, σ_e is the fold surface free energy, Δh_f is the heat of fusion per unit volume of crystal, k_B is the Boltzmann constant, and n indicates the crystallization mode (Regimes I, II or III). Regimes I and III have a theoretical value of $n = 4$, while for Regime II $n = 2$. In Regime I the nucleation rate is slow while in Regime III, it is very fast. In Regime II there is a competition between nucleation rate and solidification by chain fold.

Vyazovkin and Sbirrazzuoli [29] derive the temperature dependence of the effective activation energy of the growth rate from Eq. (17), as follows:

$$E_\alpha = U^* \left(\frac{T^2}{(T - T_\infty)^2}\right) + K_g{}^* R \left(\frac{T_m^2 - T^2 - T_m T}{(T_m - T)^2 T}\right) \quad (19)$$

This is known as the extended Hoffman–Lauritzen model. Plots of E vs. T could be fit to Eq. (19) in order to obtain the values of K_g and U^*, the Hoffman–Lauritzen parameters.

4. Results and discussion

4.1. Modified clay characterization

The modified clays obtained after the different treatments were characterized by means of X-ray diffraction and thermogravimetric analysis in order to determine their interlayer spacing and organic content, respectively (Table 1). It was observed a similar value of d_{001} peak, indicating an analogous distance between the clay platelets independently of the treatment used to modify the clay. However, the clay MAGI showed the highest organic content.

4.2. Thermal analysis of the nanocomposites

To study the effect of different kinds of clays on the thermal properties of PHB, DSC scans at 10 °C/min of PHB and its nanocomposites were performed. Fig. 2 shows the thermograms obtained from DSC data. The enthalpies of melting (ΔH_m), melting temperatures (T_m) and glass transition temperatures (T_g) were obtained from these curves and reported in Table 2. It was not observed a significant change in the melting temperature nor in the enthalpy of PHB with the clay addition. The overall crystallinity of PHB was calculated according Eq. (1). The results showed a slight diminution when 4% of all types of clay was added to the polymer. Moreover, an increment in the T_g value with the clay addition was also observed, except for the nanocomposite with the clay MAGI. It could be because of the effect of the silylation method, where the chains of the modifiers can be linked at the end of the platelets, besides being inside the galleries.

4.3. Non-isothermal crystallization of the nanocomposites

In order to analyze the effect of the clay addition on the kinetic of crystallization of PHB, DSC scans at different cooling rates from melt were performed for the PHB and its nanocomposites.

Fig. 3 shows the crystallization exotherms as a function of temperature, dH_c/dT, at several cooling rates for the PHB + 4 wt% MAI nanocomposite. It was observed that the crystallization peak becomes broader and shifts to lower temperatures with increasing the cooling rate for all the materials.

The variation of the crystallization peak temperature (T_p) with cooling rate, for the PHB/clay nanocomposites is shown in Fig. 4. The crystallization peak temperature of PHB was higher than that of the nanocomposites at all of the cooling rates studied, especially for the composite containing the clay MI. It should indicate a retardation effect of this modified clay on the PHB nucleation process.

The relative degree of crystallinity (α) was calculated from DSC data by applying Eq. (2) and converted into the time scale using

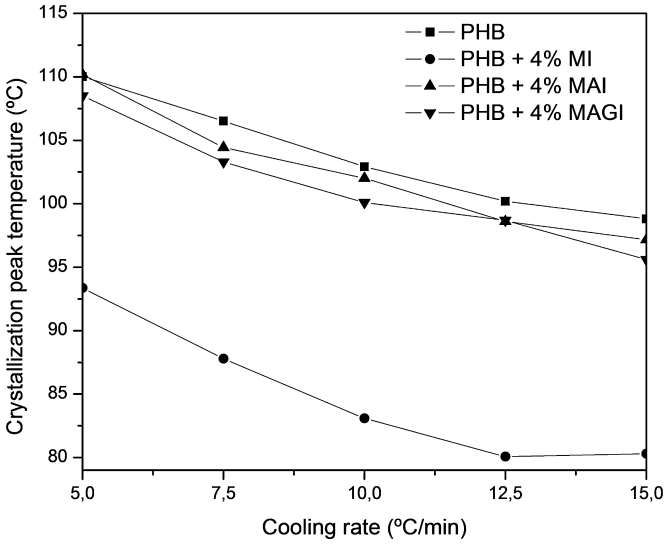

Fig. 4. Tp vs. cooling rate for PHB and its nanocomposites.

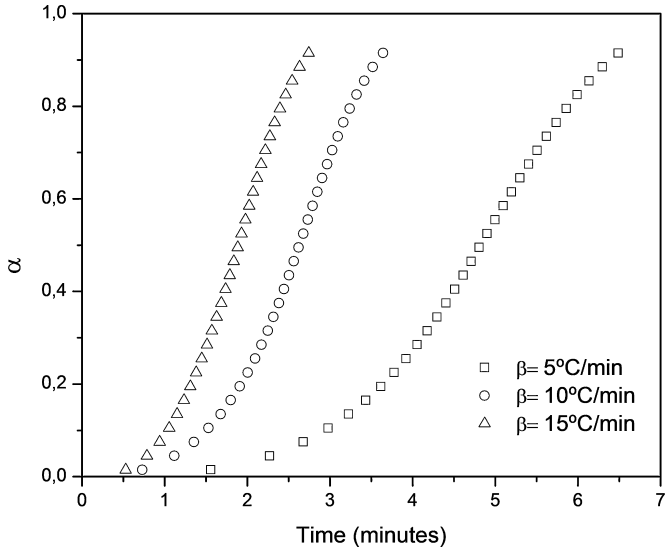

Fig. 5. α vs. time for PHB + 4% MI at different cooling rates.

Eq. (3). The plots of α at different cooling rates are shown in Fig. 5 for the PHB + 4% MI nanocomposite, as an example. It was observed that all the curves have the same sigmoidal shape, and are shifted to shorter time with increasing cooling rates for completing the crystallization. Additionally, Fig. 6 shows the plot of α vs. time for the PHB and the nanocomposites at a selected $\beta = 15\,^{\circ}$C/min, to illustrate their behavior.

To study the non-isothermal crystallization kinetics of the PHB and its nanocomposites the theory proposed by Liu–Mo, described in Section 3, was applied. Plots of $\ln(\beta)$ vs. $\ln(t)$ at a certain degree of crystallinity (20, 40, 60 and 80%) for the nanocomposite PHB + 4% MAI (Fig. 7) shows a good linearity, as also did the others studied systems. The values of $F(T)$ were determined from the intercept of the lines according to Eq. (11) and reported in Table 3. The physical meaning of $F(T)$ is the cooling rate to be employed for the system to reach a given degree of crystallinity within a unit time of crystallization. $F(T)$ values systematically increase with increasing the degree of crystallinity. The nanocomposites containing MI and MAI clays exhibited rather similar $F(T)$ values and the highest ones so, the slowest crystallization rate among the materials studied. This behavior was also observed in composites based on ZnO

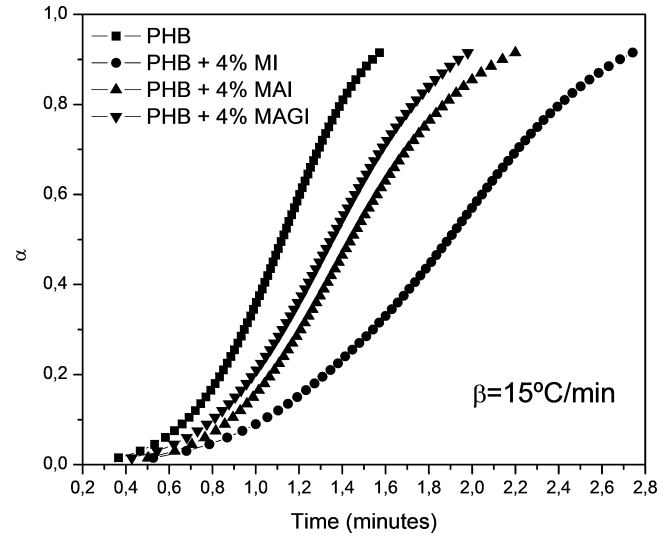

Fig. 6. α vs. time for PHB and their nanocomposites at a cooling rate of 15 °C/min.

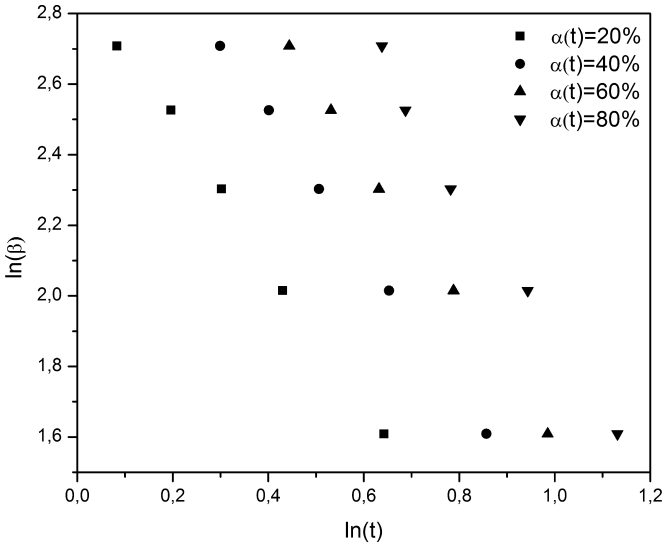

Fig. 7. Liu–Mo plots of $\ln(\beta)$ vs. $\ln(t)$ during non-isothermal crystallization of PHB + 4% MAI.

Table 3
$F(T)$ values by the Liu–Mo method, for the nanocomposites.

	F(T)			
α (%)	PHB	+4% MI	+4% MAI	+4% MAGI
20	2.49	3.05	2.89	2.73
40	2.85	3.38	3.31	3.00
60	3.07	3.57	3.59	3.18
80	3.27	3.79	4.02	3.39

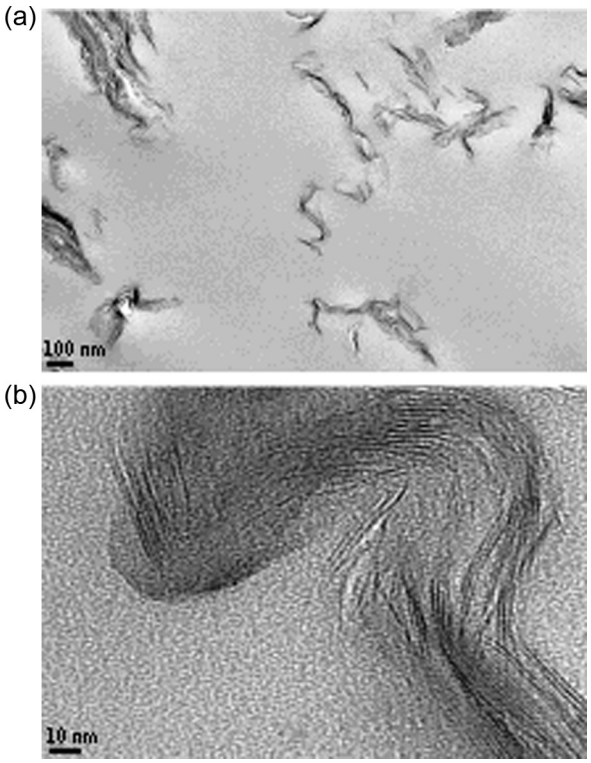

Fig. 8. TEM images of the nanocomposite PHB + 4% MAI, at different scales, (a) 100 nm, (b) 10 nm.

particles and the copolymer PHBV [32]. The platelets could hinder the mobility of the polymeric chains, thus the order during crystallization, but without varying the final degree of crystallinity [12]. On the other hand, the nanocomposite with the clay MAGI exhibited comparable $F(T)$ values to the PHB ones. This could be due to its lowest T_g value (Table 2) that allows the higher mobility of the polymeric chains, but hindered by the well dispersed clay platelets.

The clay dispersion in the nanocomposites was analyzed by DRX and TEM. Usually, these techniques are used together to determine the interlayer spacing and the clay arrangement in nanocomposites, because TEM allows the direct observation of the microstructure of the materials. The interlayer distance of the nanocomposites, calculated from DRX curves, is listed in Table 1 and a similar value was obtained among the materials. Additionally, a comparable dispersion of the clays in the PHB matrix was observed in the TEM micrographs. Fig. 8a and b shows the image of the PHB + 4% MAI at two different scales, as an example, and they revealed an intercalated structure of the clay in the polymer. So, it seems that the dispersion and distribution of the clay in the PHB were not greatly affected by the type of treatment used to modify it. All of the strategies used contribute favorably to the good dispersion of the nanoparticles in the PHB matrix.

The nucleation activity (ϕ) was also calculated in order to evaluate the effect of the different nanoparticles on the nucleation process of PHB. As it was explained in Section 3, ϕ value is close to zero when the particle is highly active, and it is close to 1 when the particle is inert. It was found (Table 2) that the modified clays do not accelerate the PHB nucleation.

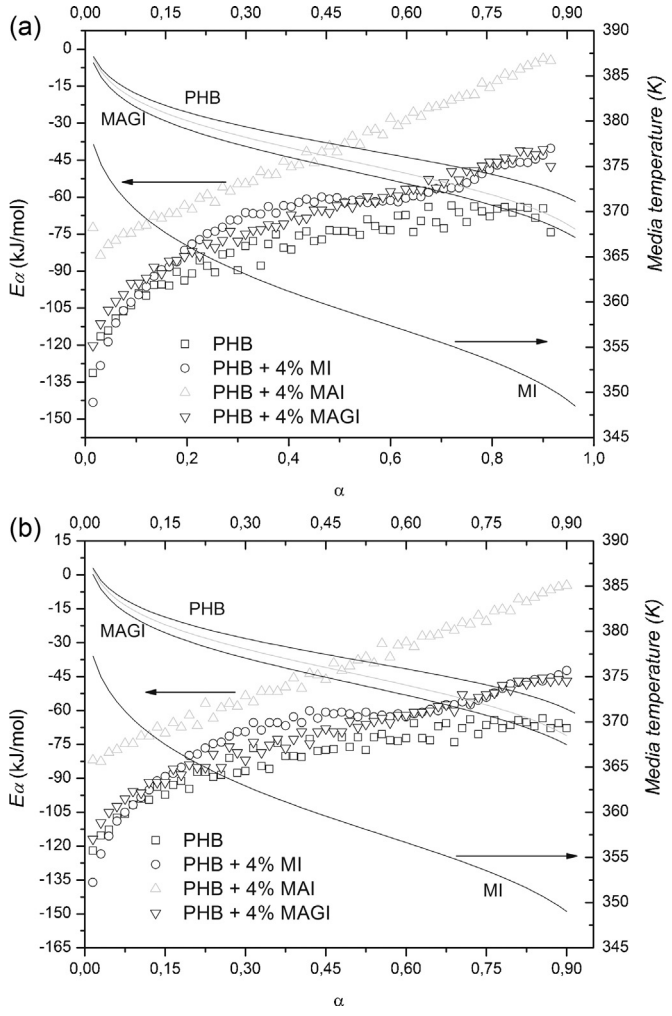

Fig. 9. Variation of the effective activation energy with the conversion for the nanocomposites and PHB, (a) by the Friedman method (b) by the Vyazovkin method.

4.4. Crystallization effective activation energy of the nanocomposites

To characterize the non-isothermal crystallization of melt polymers, an important parameter is the effective activation energy (E_α). Isoconversional methods (Friedman and Vyazovkin) were applied in order to know the variation of E_α during the crystallization process. Fig. 9a and b represents the dependence of E_α with α for the PHB and its nanocomposites obtained by those two isoconversional methods and a similar trend was observed for all materials. It was found that E_α increases with the advance of the crystallization process. E_α values were negatives in the melt crystallization region [13] and increased with the average crystallization temperature diminution (Fig. 9a and b), as it was found in a variety of polymer systems [14]. The effective activation energy must be differentiated from the true activation energy that represents the height of the energy barrier, when doing such considerations.

The addition of the clays increased E_α of the PHB in the whole range of crystallization degree, being in a higher proportion for the clay MAI. As the highest values of E_α do not imply lowest values of crystallization rate, other parameters must be found to understand the materials behavior. So, the time necessary to reach a crystallinity of 0.5 ($t_{1/2}$) at different temperatures was calculated as an approximation of the following expression:

$$t_\alpha = \frac{J[E_\alpha, T_i(t_\alpha)]}{\exp\left[\frac{-E_\alpha}{R \times T_0}\right]} \tag{20}$$

where T_0 is the desired temperature to be evaluated, t_α is the time at a given conversion value and E_α is the effective activation energy from the non-isothermal experiments at an equal conversion value. Then, the crystallization rate can be calculated as: $G \approx 1/t_{\alpha=0.5}$ [33]. Fig. 10 shows the values of G vs. temperature for the materials studied. The E_α profiles were able to be used because $t_{1/2}$ was evaluated into a range of T_0 comprising the media temperature of crystallization for each system. After that, the values of G were fitted using the Hoffman–Lauritzen model [33] in order to obtain the behavior in the whole range of temperatures (Fig. 10). It was observed that the clay addition reduces the crystallization rate of

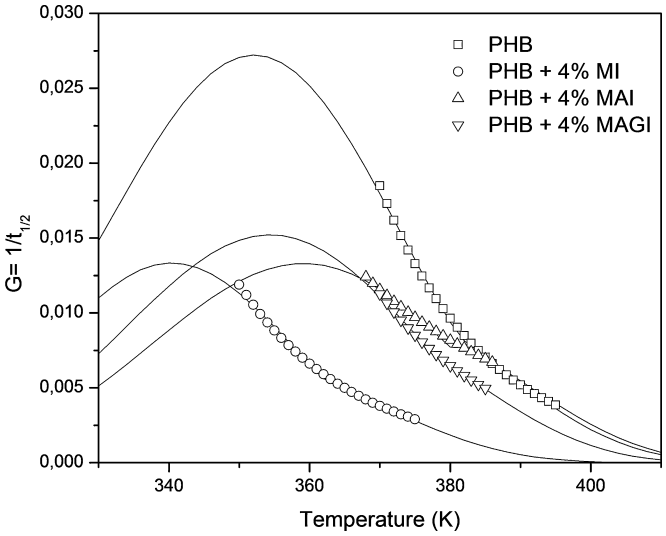

Fig. 10. Values of G obtained from the curves of E_α and the fit used Hoffman–Lauritzen model.

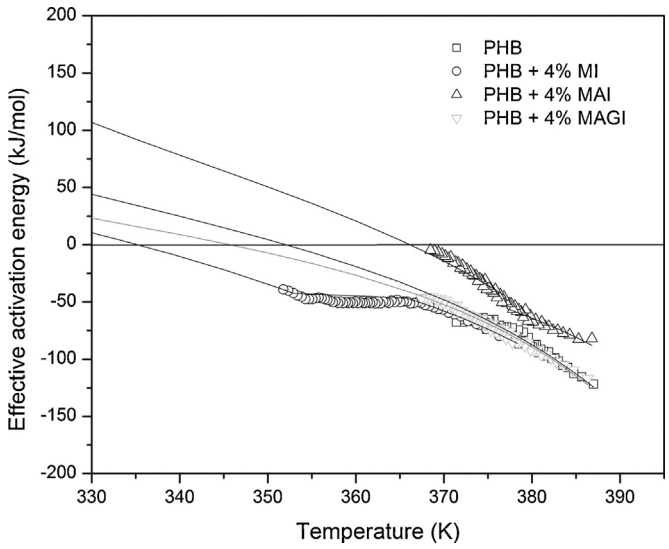

Fig.11. Experimental E_α vs. T data for the PHB and the nanocomposites. Solid lines represent a fit using Eq. (19).

Table 4
K_g *and* U^* values obtained from the modified Lauritzen–Hoffman method.

Material	Regime III			Regime II		
	$K_g \times 10^{-5}$ (K^2)	U^* (kJ mol^{-1})	Range (K)	$K_g \times 10^{-5}$ (K^2)	U^* (kJ mol^{-1})	Range (K)
PHB	3.33	5.481	378–385	–	–	–
PHB + 4% MI	3.93	3.430	351–355	2.34	2.639	367–375
PHB + 4% MAI	2.42	8.479	368–371	1.51	0.197	380–387
PHB + 4% MAGI	2.13	3.810	367–380	1.73	0.829	380–386

the PHB. Additionally, the nanocomposites showed E_α values closer to zero (Fig. 9) than the PHB, indicating that they are crystallizing at temperatures closer to their maximum crystallization rate [13].

The temperature dependence of the effective activation energy of the growth rate derived from the Hoffman–Lauritzen extended model are plotted in Fig. 11 for the different materials. It was possible to identify a change in the crystallization mechanism of the composites from this type of plots, from Regime II to Regime III. K_g and U^* values for each type of Regime estimated by fitting the corresponding data with Eq. (19), were listed in Table 4. A break point for the Regimen transition was not observed for the PHB and the values obtained were similar to the ones reported for other polymers [34]. The values of U^* at Regime II were smaller than the ones for Regime III. It could be because in Regime II the chains have more mobility to diffuse to the nuclei and continue the growth than in Regime III [13].

5. Conclusions

PHB and PHB/clay nanocomposites were obtained and characterized in order to determine their non-isothermal crystallization kinetics.

It was observed that the clay addition did not influence the melting enthalpy or the melting temperature of PHB. However, an increment of the T_g was found with the addition of the clays MI and MAI to the PHB. It was also observed that the three methods used to modify the clay favored similarly the dispersion of the nanoparticles in the PHB matrix.

The peak of the crystallization temperature of PHB diminished with the clay addition at all of the cooling rates studied. The values of $F(T)$ calculated by the Liu–Mo method indicated that the nanocomposites with MI and MAI exhibited the slowest crystallization rate among the materials studied. While the addition of MAGI did not affect the $F(T)$ of the PHB probably due to the similar T_g value between them.

The effective activation energy of the crystallization process was calculated by isoconversional methods for the PHB and the nanocomposites. It was found an increment of the E_α with the advance of crystallization, and with the clay addition. Moreover, it was found that the clay reduces the crystallization rate of PHB. It was possible to identify a change in the crystallization mechanism of the nanocomposites from Regime II to Regime III, while that break point was not observed for the PHB applying the Hoffman–Lauritzen extended model.

Acknowledgements

The authors gratefully acknowledge the support from the National Research Council of Argentina (CONICET), PIP 0014 and 0527, the National Agency for Scientific and Technological Promotion (PICT'12 1983), and the National University of Mar del Plata.

References

[1] V.P. Cyras, A. Vazquez, Ch. Rozsa, N. Galego Fernandez, L. Torre, J.M. Kenny, Thermal stability of P(HB-co-HV) and its blends with polyalcohols: crystallinity, mechanical properties and kinetic of degradation, J. Appl. Polym. Sci. 77 (2000) 2889–2900.
[2] T. Iwata, K. Tsunoda, Y. Aoyagi, S. Kusaka, N. Yonezawa, Y. Doi, Mechanical properties of uniaxially cold-drawn films of poly([R]-3-hydroxybutyrate), Polym. Degrad. Stabil. 79 (2003) 217–224.
[3] G.Q. Chen, Q. Wu, Microbial production and applications of chiral polyhydroxyalkanoates, Appl. Microbiol. Biotechnol. 67 (2005) 592–599.
[4] M.D. Sanchez-Garcia, E. Gimenez, J.M. Lagaron, Morphology and barrier properties of solvent cast composites of thermoplastic biopolymers and purified cellulose fibers, Carbohydr. Polym. 71 (2008) 235–244.
[5] A. Botana, M. Mollo, P. Eisenberg, R. Torres Sanchez, Effect of modified montmorillonite on biodegradable PHB nanocomposites, Appl. Clay Sci. 47 (3–4) (2010) 263–270.
[6] D.A. D'Amico, L.B. Manfredi, V.P. Cyras, Relationship between thermal properties, morphology and crystallinity of nanocomposites based on polyhydroxybutyrate, J. Appl. Polym. Sci. 123 (2012) 200–208.
[7] F. Bergaya, C. Detellier, J.F. Lambert, G. Lagaly, Chapter 13.0 – introduction to clay polymer nanocomposites, in: F. Bergaya, G. Lagaly (Eds.), Developments in Clay Science, Elsevier, 2013, pp. 655–677.
[8] F. Bergaya, M. Jaber, J.-F. Lambert, Clays and clay minerals as layered nanofillers for (bio) polymers, in: L. Avérous, E. Pollet (Eds.), Environmental Silicate Nano-Biocomposites, Springer, 2012, 2014, pp. 41–75.
[9] M.L. Di Lorenzo, C. Silvestre, Non-isothermal crystallization of polymers, Prog. Polym. Sci. 24 (1999) 917–950.
[10] P. Bordes, E. Pollet, S. Bourbigot, L. Averous, Structure and properties of PHA/clay nano-biocomposites prepared by melt intercalation, Macromol. Chem. Phys. 209 (2008) 1473–1484.
[11] M.L. Di Lorenzo, M. Raimo, E. Cascone, E. Martuscelli, Poly(3-hydroxybutyrate) based copolymers and blends: influence of a second component on crystallization and thermal behaviour, J. Macromol. Sci. Phys. B 40 (2001) 639–667.
[12] D.A. D'Amico, L.B. Manfredi, Cyras: crystallization behaviour of poly (3-hydroxybutyrate) nanocomposites based on modified clays: effect of organic modifiers, Thermochim. Acta 544 (2012) 47–53.
[13] S. Vyazovkin, I. Dranca, Isoconversional analysis of combined melt and glass crystallization data, Macromol. Chem. Phys. 207 (2006) 20–25.
[14] S. Vyazovkin, N. Sbirrazzuoli, Isoconversional kinetic analysis of thermally stimulated processes in polymers, Macromol. Rapid. Commun. 27 (2006) 1515–1532.
[15] S. Saengsuwan, P. Tongkasee, T. Sudyoadsuk, V. Promarak, T. Keawin, S. Jungsuttiwong, Non-isothermal crystallization kinetics and thermal stability of the in situ reinforcing composite films based on thermotropic liquid crystalline polymer and polypropylene, J. Therm. Anal. Calorim. 103 (2011) 1017–1026.
[16] W. Hao, W. Li, W. Yang, L. Shen, Effect of silicon nitride nanoparticles on the crystallization behaviour of polypropylene, Polym. Test. 30 (2011) 527–533.

[17] C. Jiang, D. Wang, M. Zhang, P.L. Shugao, M. Zhao, Effect of highly filled ferrites on non-isothermal crystallization behaviour of polyamide 6 bonded ferrites, Eur. Polym. J. 46 (2010) 2206–2215.
[18] Z. Ziaee, P. Supaphol, Non-isothermal melt- and cold-crystallization kinetics of poly(3-hydroxybutyrate), Polym. Test. 25 (2006) 807–818.
[19] Y. An, L. Dong, Z. Mo, T. Liu, Z. Feng, Nonisothermal crystallization kinetics of polyhydroxybutyrate, J. Polym. Sci. B: Polym. Phys. 36 (1998) 1305–1312.
[20] H.J. Chiu, Segregation morphology of poly(3-hydroxybutyrate)/poly(vinyl acetate) and poly(3-hydroxybutyrate-co-10% 3-hydroxyvalerate)/poly(vinyl-acetate) blends as studied via small angle X-ray scattering, Polymer 46 (2005) 3906–3913.
[21] A. Jeziorny, Parameters characterizing the kinetics of the non-isothermal crystallization of poly(ethylene terephtalate) determined by d.s.c, Polymer 19 (1978) 1142–1144.
[22] T. Ozawa, Kinetics of non-isothermal crystallization, Polymer 12 (1971) 150–158.
[23] T.X. Liu, Z.S. Mo, S. Wang, H.F. Zhang, Nonisothermal melt and cold crystallization kinetics of poly(aryl ether ether ketone ketone), Polym. Eng. Sci. 37 (1997) 568–575.
[24] S.P. Lonkar, S. Morlat-Therias, N. Caperaa, F. Leroux, J.L. Gardette, R.P. Singh, Preparation and non-isothermal crystallization behavior of polypropylene/layered double hydroxide nanocomposites, Polymer 50 (2009) 1505–1515.
[25] W.B. Xu, M.L. Ge, P.S. He, Nonisothermal crystallization kinetics of polypropylene/montmorillonite nanocomposites, J. Polym. Sci. B: Polym. Phys. 40 (2002) 408–414.
[26] S. Nandi, A.K. Ghosh, Crystallization kinetics of impact modified polypropylene, J. Polym. Res. 14 (2007) 387–396.
[27] A. Dobreva, I. Gutzow, Activity of substrates in the catalyzed nucleation of glass forming melts. II. Experimental evidence, J. Non-Cryst. Solids 162 (1993) 13–25.
[28] H.L. Friedman, Kinetics of thermal degradation of char-forming plastics from thermogravimetry, J. Polym. Sci. C: Polym. Lett. 6 (1964) 183–195.
[29] S. Vyazovkin, N. Sbirrazzuoli, Isoconversional approach to evaluating the Hoffman–Lauritzen parameters (U^* and K_g) from the overall rates of non-isothermal crystallization, Macromol. Rapid. Commun. 25 (2004) 733–738.
[30] S. Vyazovkin, A.K. Burnham, J.M. Criado, L.A. Pérez-Maqueda, C. Popescu, N. Sbirrazzuoli, ICTAC kinetics committee recommendations for performing kinetic computations on thermal analysis data, Thermochim. Acta 520 (2011) 1–19.
[31] S. Vyazovkin, N. Sbirrazzuoli, Isoconversional analysis of calorimetric data on nonisothermal crystallization of a polymer melt, J. Phys. Chem. B 107 (2003) 882–888.
[32] W. Yu, C.-H. Lan, S.-J. Wang, P.-F. Fang, Y.-M. Sun, Influence of zinc oxide nanoparticles on the crystallization behavior of electrospun poly(3-hydroxybutyrate-co-3-hydroxyvalerate) nanofibers, Polymer 51 (2010) 2403–2409.
[33] J.D. Hoffman, G.T. Davies, J.I. Lauritzen, Treatise on Solid State Chemistry: Crystalline and Non-crystalline Solids, Plenum, New York, 1976.
[34] G.Z. Papageorgiou, D.S. Achilias, D.N. Bikiaris, Crystallization kinetics of biodegradable poly(butylene succinate) under isothermal and non-isothermal conditions, Macromol. Chem. Phys. 208 (2007) 1250–1264.